JOURNAL OF ENGINEERED FIBERS AND FABRICS

Original Article

Journal of Engineered Fibers and Fabrics
Volume 14: 1–14

DOI: 10.1177/1558925019829049
journals.sagepub.com/home/jef
SAGE

Effect of fixation conditions on yellowing behavior of cellulose powder–coated fabrics

Gizem Manasoglu[1], Mehmet Kanik[1] and Kenan Yildirim[2]

Abstract

In this study, the yellowing behavior of cellulose powders, which is applied to pretreated polyester woven fabrics with concentrations of 100 g/kg by knife coating technique, was investigated. After drying process, coated fabrics were cured at different conditions to determine the effects of the curing temperature and time on yellowing behaviors. The yellowness–whiteness of coated fabrics was measured with a spectrophotometer according to ASTM E313. As the curing temperature and time increase, yellowing effect was more observable. However, the effect of temperature increase is found to be more significant than the increase in curing duration in terms of more observed yellowness. In order to investigate the reason of yellowing, cellulose powder samples were heated in drying oven at three different heating temperatures (130°C, 150°C, and 170°C) for three different heating periods (3, 5, and 7 min). Then, thermal gravimetric analysis and Fourier transform infrared spectroscopy analysis of powder samples were performed for each temperature–period combinations. No ring-opening reaction on the cellulose group was found in the Fourier transform infrared spectroscopy analysis. However, the changes in the spectra can be attributed to the chain breakage in the cellulose macromolecules as well as water loss from the molecular structure during the heating process. Microscopic and scanning electron microscopic analysis was carried out to see any surface change on the fiber and coated fabric. There was no detectable surface change on the fiber and coated fabric surface, apart from a color change on the fabric surface.

Keywords

Cellulose powder, Fourier transform infrared spectroscopy, temperature, thermal gravimetric analysis, yellowing, textile coating

Date received: 2 August 2018; accepted: 9 January 2019

Introduction

Advances in polymer and textile technology have led to the phenomenal growth in the application of coated fabrics for many diverse end uses. Coated fabrics find an important place among technical textiles and are one of the most important technological processes in the modern industry.[1] Coated fabrics are engineered composite materials, produced by a combination of a textile fabric and a polymer coating applied to the fabric surface.[2] With the developments in polymer and material technology, coated textiles can be used in more sophisticated applications such as aerospace, automotive, electronic, geotextile, military, and air conditioning.[3] Cellulose is considered to be the most abundant polymer derived from biomass.[4] It is a linear syndiotactic homopolymer of β-(1→4)-glycosidic bonds linked to D-anhydroglucopyranose.[5] It is renewable, eco-friendly, low cost, low density, and contains hydroxyl groups on the surface, which allow it to form strong

[1]Bursa Uludağ University, Bursa, Turkey
[2]Bursa Technical University, Bursa, Turkey

Corresponding author:
Gizem Manasoglu, Uludag University, Nilüfer, 16059 Bursa, Turkey.
Email: gmanas@uludag.edu.tr

Table 1. Properties of coating chemicals.

Chemical	Property
Binder (Tubicoat HC 30; CHT)	Self-cross-linking acrylate-based copolymer, anionic
Fixation agent (Fixierer HT; CHT)	Low formaldehyde melamine resin, nonionic
Synthetic thickener (Tubivis Star; CHT)	Ammonium salt of carboxylic acid polymers, anionic
Anti-foam agent (Hansa Antifoam 1010; CHT)	Emulsion of modified siloxanes, nonionic
Liquid ammonia	25%
Water	Soft water (reverse osmosis)

hydrogen bonds with oxygen atoms on the same or on a neighbor chain.[6] As one of the most common and renewable organic polymers, cellulose is an important raw material for several industries such as textiles, papers, foods, cosmetics, and biomaterials.[7]

Application of engineered nanomaterials has offered a new generation of environment-friendly coating materials in textile industries. Fibers used in the textile industry are notably improved by nanotechnology; one example is nanocellulose, which combines low cost, lightweight, electric conductivity, environment-friendly resources, and high resistance, thus opening an immensely vast scope of possible applications.

Microcrystalline cellulose is extracted by acid hydrolysis from the short fibers formed from snap of long fibers in the spinning systems. The powder produced was coated with natural or synthetic fabrics. They offer possibilities such as improved durability, self-cleaning, and water- or dirt-repellent features.[8]

Functional cellulose products can be used in many fields such as floor covering, automotive, filtration, road construction, carrier materials, and polyurethane (PU) synthetic leather industry.[9,10]

Coating systems based on natural polymers (e.g. cellulose) are neither used nor available due to the lack of suitable coating progenitors. However, such "green" coatings based on natural polymers such as cellulose would provide interesting material properties and simplify waste disposal. Furthermore, coating materials based on cellulose would complete the spectrum of the coating properties available so far with the specific qualities of cellulose and provide coatings with good adhesion to cellulosic and other textiles, for example, poly(ester)s or poly(amide)s.[11] Kale et al.[12] researched the effect of cellulose coating on dyeing and stiffness characteristics of cotton fabrics. d'Eon et al.[13] investigated conditions to deposit cellulose nanocrystal (CNC) films onto polypropylene (PP) by spin coating and they studied the adhesion, mechanical property, and oxygen permeability properties of the CNC-coated PP films. El Fattah et al. extracted nanocrystalline cellulose (NCC) and micro-powdered cellulose (MPC) from rice straw. The resultant cellulosic materials were applied as green reinforcement fillers in the PU coating.[6] Thermal behavior and degradation of cellulose are also studied in the literature. Brillard et al. investigated thermal degradation of different used cotton samples under an inert atmosphere (N_2) and under air (20% O_2, 80% N_2) with different temperature ramps (5°C–50°C min^{-1}). The thermal degradation of pure cellulose can also be analyzed for comparison, as cotton is mainly composed of cellulose.[14] Szcześniak et al.[15] also studied glass transition temperature and thermal decomposition of cellulose powder using differential scanning calorimetry (DSC), differential thermal analysis (DTA), and thermal gravimetry (TG). Teodorovic et al. investigated the thermal characteristics of cellulose samples with different structures. The thermal behavior of the samples was studied using Perkin Elmer TGS-2 and DSC-2 instruments.[16]

Although CNCs have been studied in the literature for coating applications, potential of the cellulose powder to be a coating material is not investigated thoroughly. In this study, cellulose powder (i.e. inexpensive compared to CNCs) coated with polyester fabrics was cured at different temperatures and periods during which color changes on the coated areas were observed. Yellowness–whiteness values of coated samples were measured. In addition, cellulose powders used as a filling material were heated in drying oven at three different temperatures during three different periods. Thermal gravimetric analysis (TGA) and Fourier transform infrared spectroscopy (FTIR) analysis were performed and compared with uncured standard cellulose powder.

Experiment

Materials

A satin weave polyester fabric which was supplied by the Kırayteks Inc. (Bursa, Turkey) was used in the experiments. The warp and weft densities of the satin weave 100% polyester fabrics were 47 ends/cm and 23 picks/cm. The weight of polyester fabric was 248 g/m^2. The wood-sourced cellulose powders were supplied from JRS Group (Rosenberg, Germany). The powder's cellulose content was 99.5 wt%. It had 120 µm average fiber length and 25 µm fiber thickness. Its bulk density was 150–185 g/L. Binder, fixation agent, thickener, and anti-foam agent were supplied from CHT Chemistry (Turkey). Table 1 shows the properties of coating chemicals.

Table 2. Stock paste composition.

Stock paste	
Binder	350 g
Water	580 g
Fixation agent	25 g
Synthetic thickener	35 g
Anti-foam agent	5 g
Ammonia	5 g
Total	1000 g

Method

Preparing stock and coating pastes. The stock paste was prepared with mixing materials that are shown in Table 2. The pH value of the paste was in the range of 9.5–10. Viscosity values were varied in the range of 5600 ± 500 cP. Coating pastes were prepared by adding cellulose powder as a filling material and deficient amount of thickener to the stock pastes. Cellulose powder was used in 100 g/kg concentration rate. Viscosity values of coating pastes were varied in the range of 9000 ± 500 cP. Brookfield RVT Analog Viscometer was used for viscosity measurements.

Coating

Pre-treated (washed and thermofixed at 180°C) 100% polyester woven fabrics were coated with cellulose powders by knife coating technique on a laboratory-type coating machine (Rapid Auto Coating).

In order to examine the effect of cellulose powder on the yellowing behavior of coatings after the curing process, control-coated fabrics were prepared. Fabrics were coated with stock paste without adding cellulose powder. Coatings were made according to knife over roll principle and a sharp pointed knife was used. The distance between the knife and fabric was arranged as 0.5 mm and it was constant for every sample.

Drying and fixation

After coating process, samples were dried at 110°C for 5 min and they were cured at different temperatures and periods on a laboratory-type steamer (Rapid H-TS-3). In order to measure the effect of temperature on the yellowing behavior of the coated fabrics, five different temperatures (130°C, 140°C, 150°C, 160°C, and 170°C) were tested, while the curing period was kept constant at 3 min. In order to measure the effect of time on the yellowing behavior of the coated fabrics, five different periods (2, 3, 4, 5, and 6 min) were tested, while the curing temperature was kept constant at 140°C. The coating recipes were same for both conditions and two coated fabrics were tested for each temperature/period value.

Table 3. Sample codes of heated cellulose powders.

Sample code	Heating conditions
Cellulose 1	Uncured
Cellulose 2	130°C—3 min
Cellulose 3	130°C—5 min
Cellulose 4	130°C—7 min
Cellulose 5	150°C—3 min
Cellulose 6	150°C—5 min
Cellulose 7	150°C—7 min
Cellulose 8	170°C—3 min
Cellulose 9	170°C—5 min
Cellulose 10	170°C—7 min

After coating process, the control-coated fabrics were cured at same temperature/period conditions to compare with cellulose powder–coated fabrics.

Thermal process of cellulose powders

Cellulose powders used as a filling material were heated in drying oven. Three different heating temperatures (130°C, 150°C, and 170°C) were tested for three different heating periods (3, 5, and 7 min). TGA and FTIR analyses of the samples coded for each temperature–time combination and the standard powder which was uncured were performed. Sample codes are listed in Table 3.

Yellowness–whiteness measurements

Konica Minolta CM-3600D model spectrophotometer was used to measure the yellowing of the coated fabrics and cellulose powders which were cured at different temperature and period conditions. The yellowness and whiteness index values of the samples were measured in order to determine the rate of yellowing on the coatings and cellulose powders.

Among cellulose powder–coated fabrics, the fabric that was dried but was not cured was used as standard fabric in measurements.

Among control-coated fabrics, the fabric that was coated with stock paste and dried but was not cured was used as standard fabric in measurements.

Among cellulose powders, uncured powder sample that coded as Cellulose 1 was standard in measurements. The treated samples at different heating conditions (from Cellulose 2 to Cellulose 10) were compared with the Cellulose 1 and each other.

The yellowness–whiteness values of the standard samples were taken and the results of other treated fabrics and cellulose powders were compared to determine the amount of yellowing. The yellowness and whiteness values were measured according to ASTM E313 and Stensby (D 65) standards, respectively. Two measurements were taken for

Table 4. Measured average yellowness and whiteness values of the cellulose powder–coated samples cured at different temperatures.

Sample code	Curing temperature	Yellowness (ASTM E313)	Whiteness (Stensby)
Standard	–	3.39	80.53
130/3	130°C	9.87	67.77
140/3	140°C	11.58	63.67
150/3	150°C	17.90	50.76
160/3	160°C	23.40	40.17
170/3	170°C	37.88	18.83

each sample. The differences between the yellowness–whiteness values according to the standard ones were determined by taking the average of the results of two samples subjected to the same curing conditions.

Optical microscopy

Optical microscopy images of cellulose powders that were heated at different conditions were taken with Leitz Dialux 20 EB with an objective of 160×. Optical microscopy images of cellulose powder–coated fabrics that were cured at different temperature/period conditions were taken with Mshot MS60 digital microscope.

Scanning electron microscopy

Scanning electron microscopic (SEM) images of cellulose-coated fabrics that were cured at different conditions and cellulose powders that were heated at 130°C, 150°C, and 170°C for 7 min were taken with Zeiss EVO40 scanning electron microscope. Magnification rate was chosen as 500× for fabrics and 1000× for powders.

TGA

Perkin Elmer STA 600 model thermo-gravimetric analyzer was used for TGA. The initial and the final temperatures of TGA were 50°C was 900°C, respectively; the heating rate was 30°C/min; purge gas was nitrogen until 600°C, afterward changed to oxygen; and the amount of test specimen was about 5 mg.

FTIR analysis

FTIR spectra were obtained using Thermo Scientific-Nicolet i550 FTIR model device with Smart Orbit-Diamond ATR attachment. The spectra were taken between 4000 and 550 cm^{-1} wavenumbers with a resolution of 4 cm^{-1}. The absorption bands in FTIR spectra were analyzed by Omnic 9 software. An average of 16 scans was accumulated for each spectrum. All FTIR spectra were taken under the condition that same pressure was applied onto all samples.

Results and discussion

In the preliminary tests, it has been observed that yellowing occurs in coatings especially during curing at high temperatures. The effects of curing temperature and period on yellowing behavior were investigated. Two samples were tested for each different curing condition and their averages were taken.

Yellowness–whiteness results of coated fabrics at different temperatures

The yellowness and whiteness results of fabrics cured at different temperatures are shown in Table 4. The results show that during the 3 min curing period, as the temperature rises from 130°C to 170°C, the amount of yellowing in coatings increases significantly and whiteness decreases accordingly. At a curing temperature of 130°C, the yellowness value of the coating increased by 6.48 units compared to the standard sample. The difference reached to 34.49 units when the temperature increased to 170°C. The whiteness value was obtained as 67.77 at 130°C temperature which decreased to 18.83 when the temperature reached 170°C. The values in the table show that there is no significant difference between the yellowing amounts which occurred at 130°C and 140°C temperatures. Because of this, considering the advantage of working at higher temperatures in terms of production speed, 140°C curing temperature was approved for following tests.

In order to determine how much of the yellowing was caused by cellulose powders and how much of it was caused by coating chemicals, cellulose powder–free control coatings were performed and cured at different conditions.

The yellowness and whiteness results of control-coated fabrics cured at different temperatures are shown in Table 5. The yellowness value of the coating increased by 2.96 units compared to the control-coated standard sample at a curing temperature of 130°C. The difference reached to 12.84 units when the temperature increased to 170°C. According to the results, yellowness values increased with the increase in curing temperature. However, these increases were not as high as those

Table 5. Measured average yellowness and whiteness values of the control-coated samples cured at different temperatures.

Sample code	Curing temperature	Yellowness (ASTM E313)	Whiteness (Stensby)
CC Standard	–	3.44	81.61
CC 130/3	130°C	6.40	73.70
CC 140/3	140°C	7.29	71.26
CC 150/3	150°C	8.88	67.32
CC 160/3	160°C	11.41	60.61
CC 170/3	170°C	16.28	48.42

Table 6. Measured average yellowness and whiteness values of the cellulose powder–coated samples cured at 140°C for various curing periods.

Sample code	Curing period	Yellowness (ASTM E313)	Whiteness (Stensby)
Standard	–	3.39	80.53
2/140	2 min	11.23	64.77
3/140	3 min	10.42	66.20
4/140	4 min	12.31	62.23
5/140	5 min	13.78	59.28
6/140	6 min	16.63	52.95

Table 7. Measured average yellowness and whiteness values of the control-coated samples cured at 140°C for various curing periods.

Sample code	Curing period	Yellowness (ASTM E313)	Whiteness (Stensby)
CC Standard	–	3.44	81.61
CC 2/140	2 min	6.33	73.82
CC 3/140	3 min	6.79	72.56
CC 4/140	4 min	7.31	71.35
CC 5/140	5 min	7.75	69.88
CC 6/140	6 min	8.33	68.72

samples coated with cellulose powder. For instance, according to results in Tables 4 and 5, while the yellowness value of 170/3 coded sample was 37.88, this value was 16.28 for CC 170/3 coded sample. This situation was similar to other curing temperatures.

These results not only indicate that the yellowing effect on the coated fabrics is largely due to the yellowing of cellulose powders but also show that other coating chemicals have a significant contribution to yellowing.

Yellowness–whiteness results of coated fabrics at different periods

The yellowness and whiteness results of fabrics that were cured at different periods are shown in Table 6.

The average values on the table show that the increase in curing period also increases the yellowing rate of coatings and decreases the whiteness values proportionally. However, the effect of yellowness depending on the increase in time is not as rapid as the increase in temperature. While the average yellowness value obtained after 2 min curing was 11.23 when the curing period was 6 min, the value increased to 16.63. The whiteness value of the standard sample, which was 80.53, decreased to 64.77 after 2 min curing and to 52.95 after 6 min curing.

The results in Table 6 show that the whiteness losses that occurred during curing times of 2, 3, and 4 min are too close to each other and that the small differences between them can also occur in the frame of the experiment mistakes. If the yellowness value after 3 min is low compared to 2 min, it may be a result of a fluctuation in the curing temperature at this point.

The yellowness and whiteness results of control-coated fabrics cured at different periods are shown in Table 7. The yellowness value of the coating increased by 2.89 units compared to the control-coated standard sample at a curing period of 2 min. The difference according to yellowness value of standard increased to 4.89 at the end of the 6 min curing period. According to results, yellowness values increased and whiteness values decreased with the increase in curing period.

Table 8. Measured average yellowness and whiteness values of the cellulose powders heated at different conditions.

Sample code	Heating conditions	Yellowness (ASTM E313)	Whiteness (Stensby)
Cellulose 1	Uncured	7.43	69.42
Cellulose 2	130°C—3 min	7.60	68.78
Cellulose 3	130°C—5 min	7.68	68.62
Cellulose 4	130°C—7 min	7.75	68.19
Cellulose 5	150°C—3 min	7.67	68.66
Cellulose 6	150°C—5 min	7.95	68.47
Cellulose 7	150°C—7 min	8.22	67.81
Cellulose 8	170°C—3 min	7.96	68.13
Cellulose 9	170°C—5 min	8.57	66.98
Cellulose 10	170°C—7 min	8.79	66.60

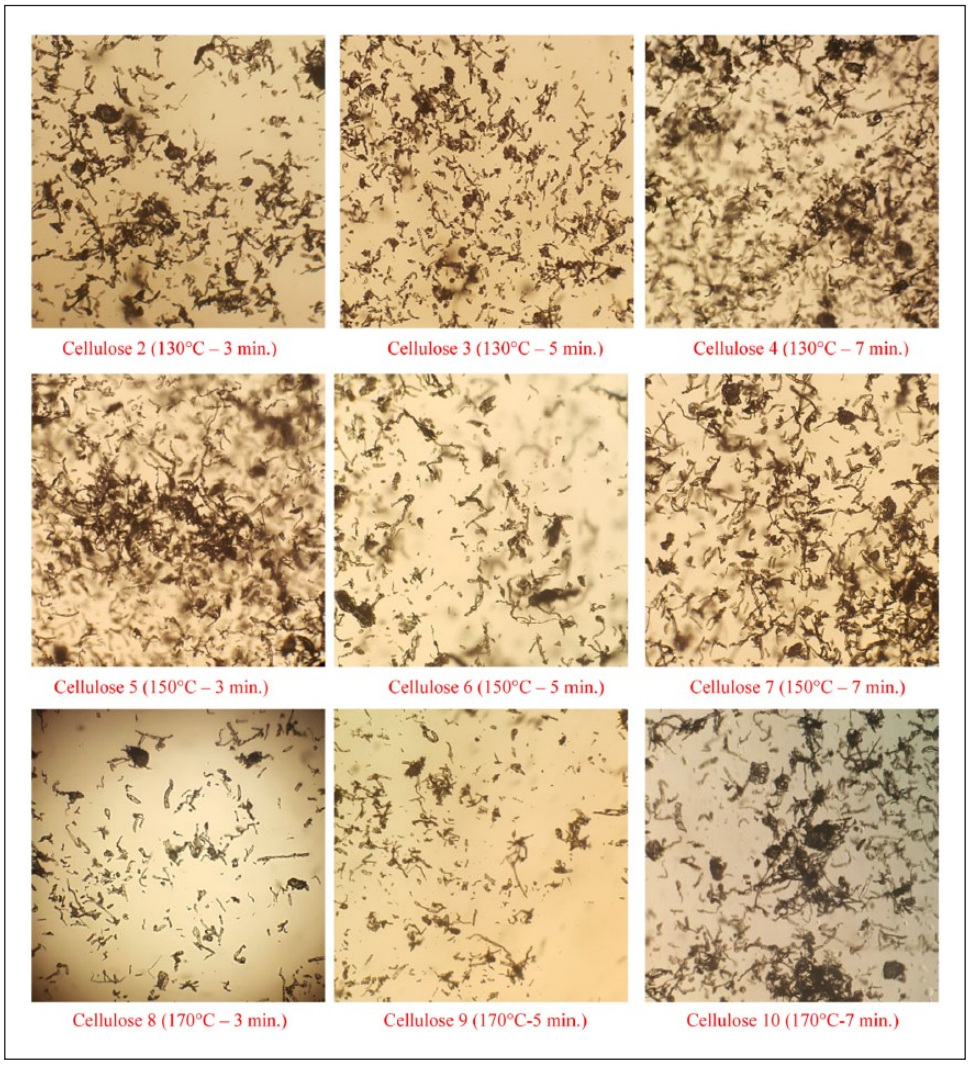

Figure 1. Optical images of cellulose powders heated at different conditions.

Tables 6 and 7 show that the effect of cellulose powders on the yellowing behavior of coatings was higher than other coating chemicals for different curing periods.

Finally, when all values were examined, the effect of curing temperature on yellowing was much more obvious than the curing period.

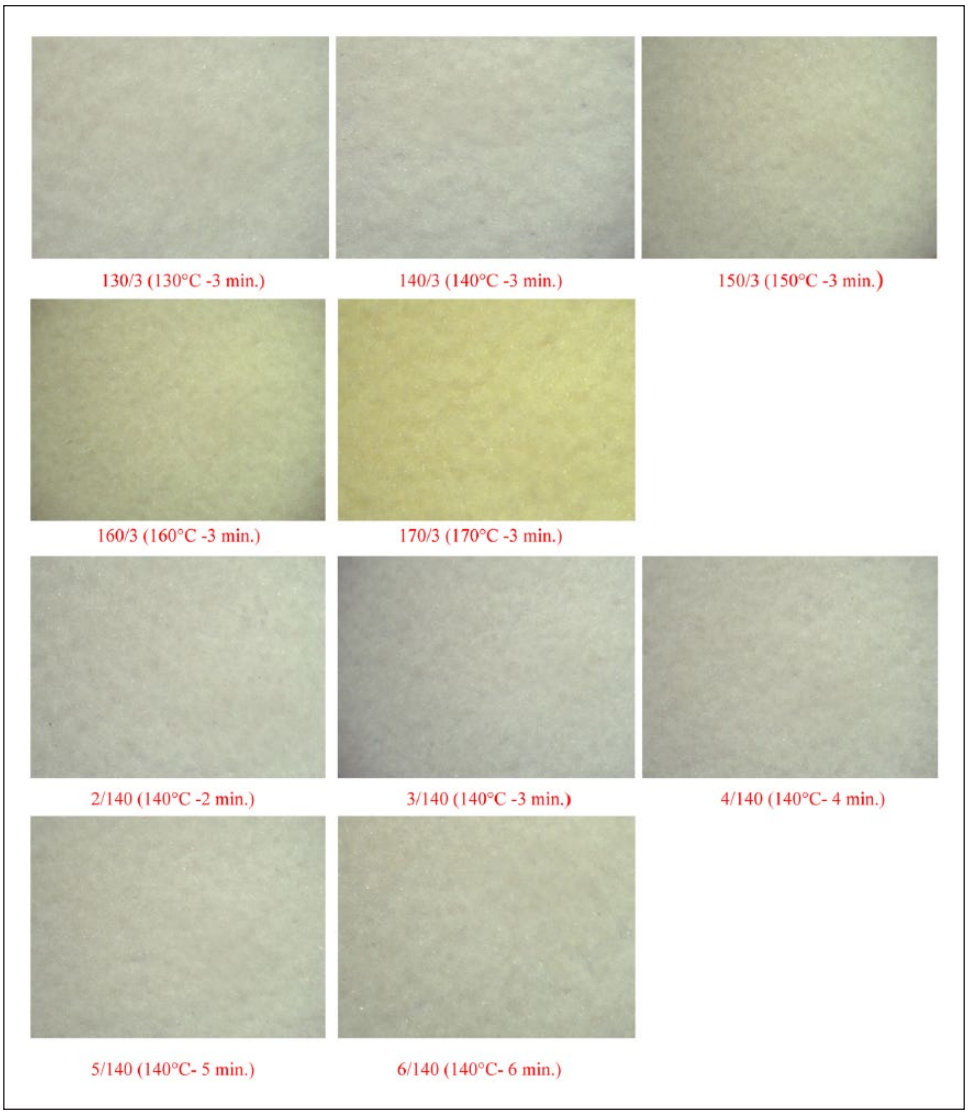

Figure 2. Optical images of cellulose powder–coated fabrics cured at different conditions.

Yellowness–whiteness results of cellulose powders

The yellowness and whiteness results of cellulose powders heated at different temperatures and periods are shown in Table 8. The results show that yellowness values were increased and whiteness values were decreased with the increase in heating temperature and period.

According to these results, it was thought that the yellowing of coated fabrics after curing may be caused by the synergistic effect of cellulose powders and coating chemicals. According to Table 8, the yellowing of dry cellulose powders remained at a minor level despite long-term heat treatment at high temperature (170°C—7 min).

Optical microscopy images

Optical images of the cellulose powders heated at different temperatures for different periods are shown in Figure 1. There was no significant change in the shape of cellulose powders with increasing temperature or time effect.

Optical images of the fabrics that were coated with cellulose powder and cured at different conditions are shown in Figure 2. In accordance with the results in Tables 4 and 6, yellowing was observed in the coatings with the increase in curing temperature and period. Color differences between fabrics (2/140–6/140) that were cured at constant curing temperature for different periods were not very significant. However, color differences between fabrics (130/3–170/3) that were cured at

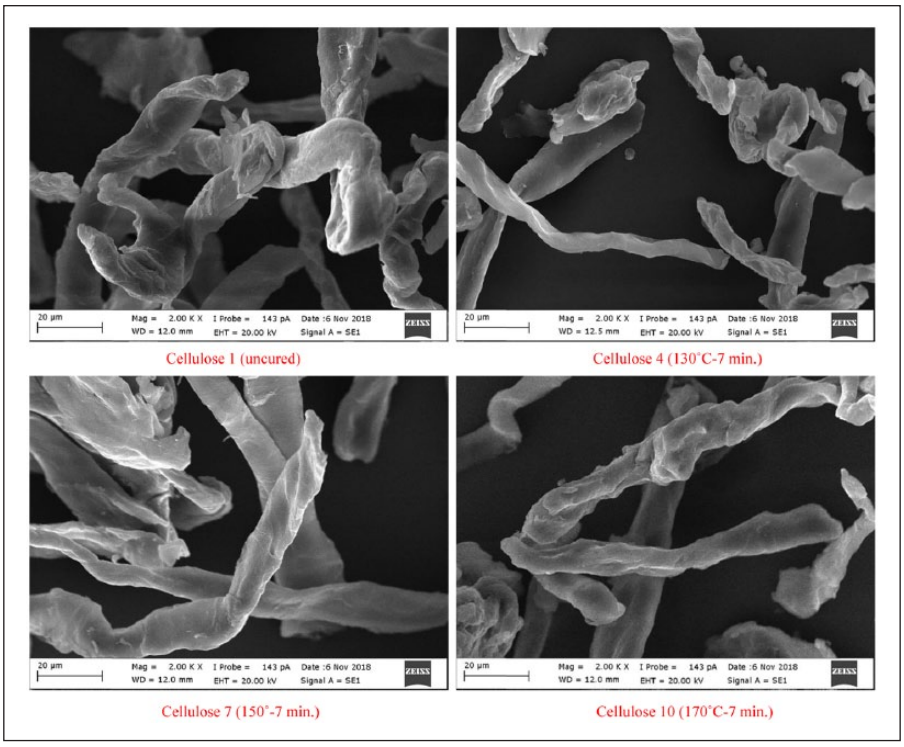

Figure 3. SEM images of cellulose powders that were cured at different conditions.

different curing temperatures for constant period could be easily observed.

SEM images

When the images in Figure 3 were examined, no significant difference was observed in the form of cellulose powders after the heating process.

Similarly, according to images in Figures 4 and 5, it was evaluated that a deformation or important difference did not occur on coating surfaces with the increase in curing temperature/period. Therefore, the change was thought to be limited with yellowing only.

FTIR analysis results

FTIR spectrum of all samples (baseline correction was done) looks like cellulose FTIR spectrum (Figures 6 and 7).[14,17] The broad peak on 3333 cm^{-1} and the broad but less intensive peak on 1639 cm^{-1} are related to OH group of cellulosic molecule structure and water molecule. The peak series between 2819 and 2849 cm^{-1} belong to CH_2 groups in the cellulose structure. The peak series between 1455–1313 cm^{-1} and 1161–898 cm^{-1} are related to cellulosic molecular structure. These peaks are fingerprint of the cellulose. These peaks are related to C-H, C-O, and C-O-C deformation, bending, or stretching vibrations of cellulose molecule.[18,19] While the peak at 898 cm^{-1} is related to amorphous region in cellulose, the peaks at around 1425 cm^{-1} are associated with the crystalline structure. The peak at 1455 cm^{-1} is related to CH_2 bending vibration.[19–21] After processing of cellulose in the high-temperature condition within the limits of this study, no new peak formation was observed, but some peak intensities were changed. The amount of change of the area of OH peak both at 3333 and 1639 cm^{-1} was nearly the same. The sequence from big area to small area according to OH peaks corresponds to cellulose 1, 8, 2, 7, 4, 3, 10, 6, 5, and 9. The lowest areas were 4866 for OH at 3333 cm^{-1} peak and 299 at 1639 cm^{-1} peak, the highest areas were 6680 at 3333 cm^{-1} peak and 412 at 1639 cm^{-1} peak. It can be determined from the change in OH peak area that cellulose lost water during heating. The OH group is found both in the cellulose molecule and in the water molecule in the cellulose crystal structure. Thus, the change in OH peak is not only related to the depletion of water in the cellulose crystal structure but also to the change in OH group in the cellulose molecule structure. Crystalline structures are more regular, so the number of macromolecules in the unit volume is higher. Because of these OH groups are more intense, by changing this density, the OH peak area in the FTIR spectrum changes. In another case, the amount of water contained in the cellulosic material varies depending on the cellulose morphology.[22,23] For these reasons, the relationship between the change in peak area at 3300 cm^{-1} and the increase in heating temperature is not clearly seen. The peak between 3600 and 2750 cm^{-1} is related to OH group based on the O-H and C-H stretching vibration.[24]

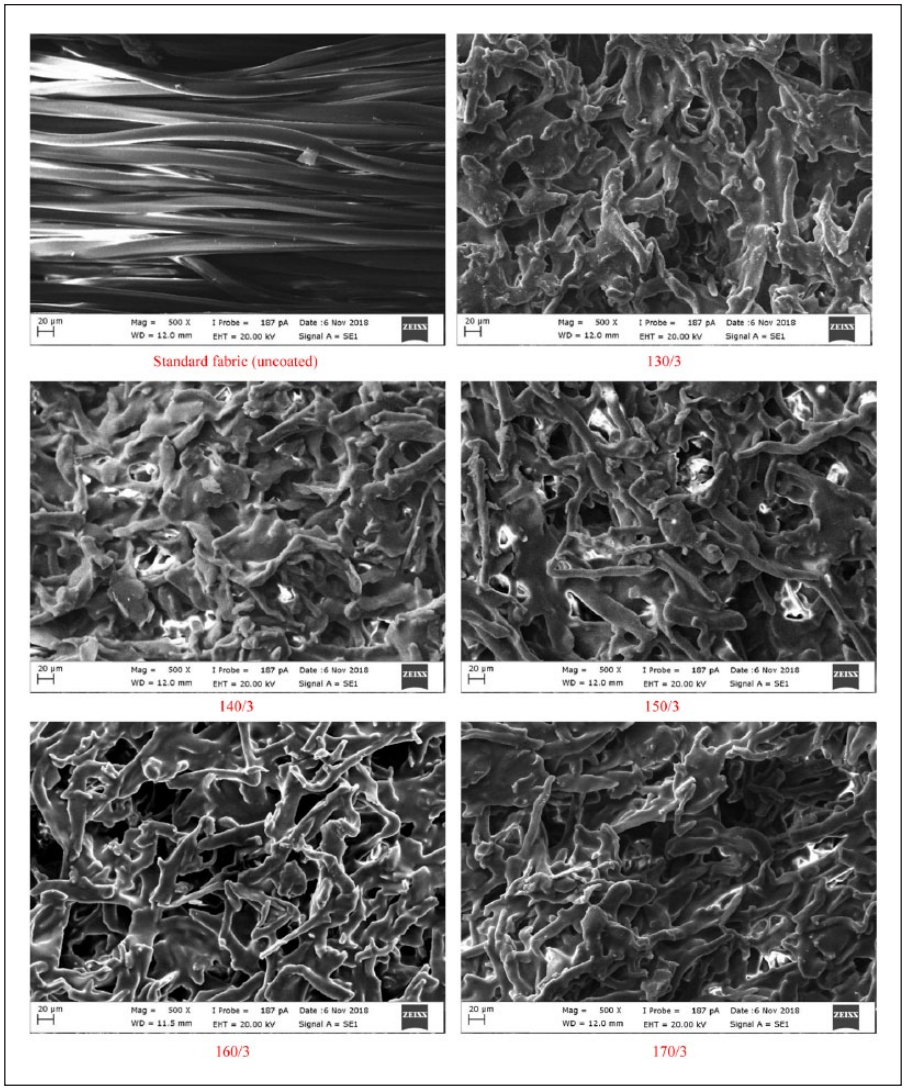

Figure 4. SEM images of cellulose powder–coated fabrics that were cured at different temperatures.

The peak at 3432 cm^{-1} is associated with intramolecular hydrogen bond vibration. Another intramolecular hydrogen bond in cellulose normally occurs at 3342 cm^{-1}. The two characteristic bands assigned to the two crystalline cellulose allomorphs, cellulose Iα and cellulose Iβ, also occur in the region of 3220–3280 cm^{-1}. The peak at 3221 cm^{-1} is assigned to the intramolecular hydrogen bonds present only in triclinic Iα cellulose, whereas the band at close to 3277 cm^{-1} is proportional to the amount of monoclinic cellulose Iβ.[18,25]

The changes in 1159 cm^{-1}, which are specific peak of cellulose macromolecule, also indicate the presence of this side effect. The peak at 1159 cm^{-1} is related to C-O-C group in cellulose I and cellulose II. Any decrease in the peak intensity implies that there is a defect on the bond of this group.[19,26] C-O-C group places in the aromatic structure and between monomers in the cellulose structure.

Ring opening in the cellulose structure gives either carboxyl or aldehyde group.[27,28] Both groups give peak at 1710–1685 cm^{-1} on the FTIR spectrum.[17,29] There was no ring-opening reaction observed in the cellulose structure during heating, as no peak was formed at around 1710 cm^{-1} on the FTIR spectra. The irregularity of the change in the OH peak areas and decomposition beginning temperature on the TGA thermogram imply that there may be a breakage in the chain of cellulose macromolecule. The thermal stability increases as the molecular weight increases.[26,30] The change in the peak height at 1105 cm^{-1} on the FTIR spectra with temperature increase also supports this proposal. This peak is related to C-O stretch and C-C bonds in the cellulose macromolecule.[31] The tendency of decrease in the area of the peak at 896 cm^{-1} with increasing temperature was the other proof for chain breakage in the cellulose macromolecule. This peak is related to C-O-C bond

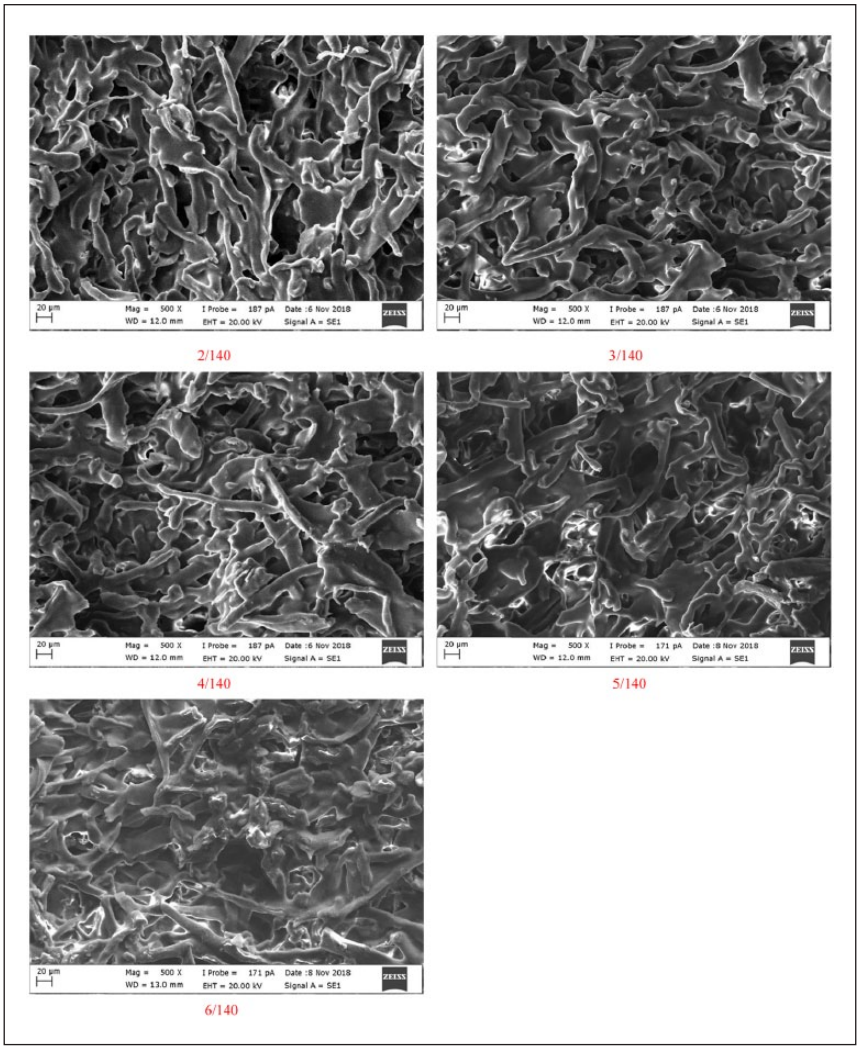

Figure 5. SEM images of cellulose powder–coated fabrics that were cured at different periods.

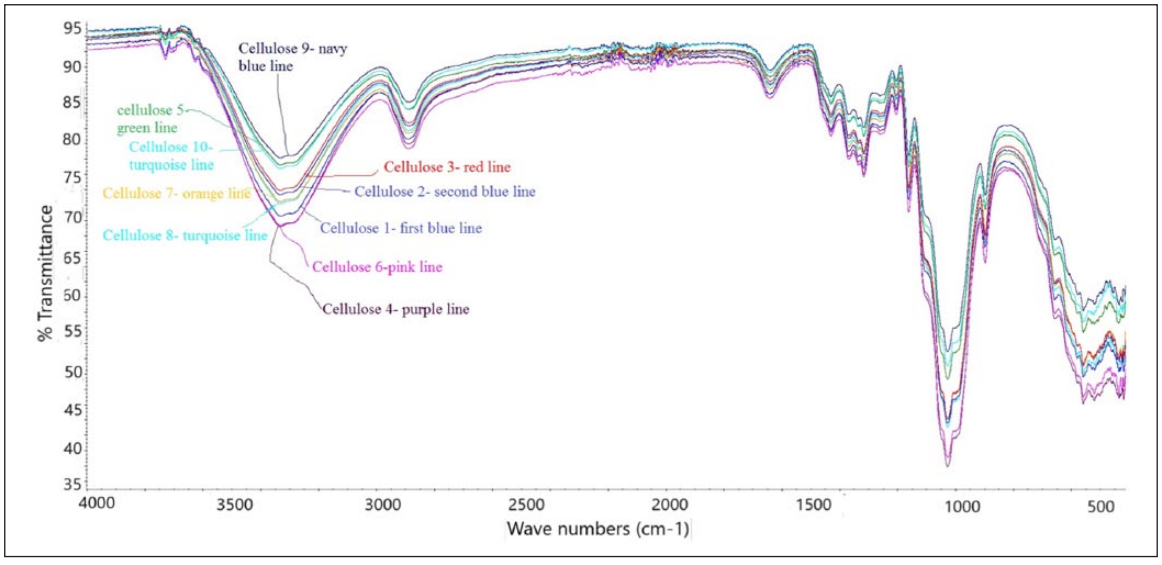

Figure 6. FTIR spectra of all samples.

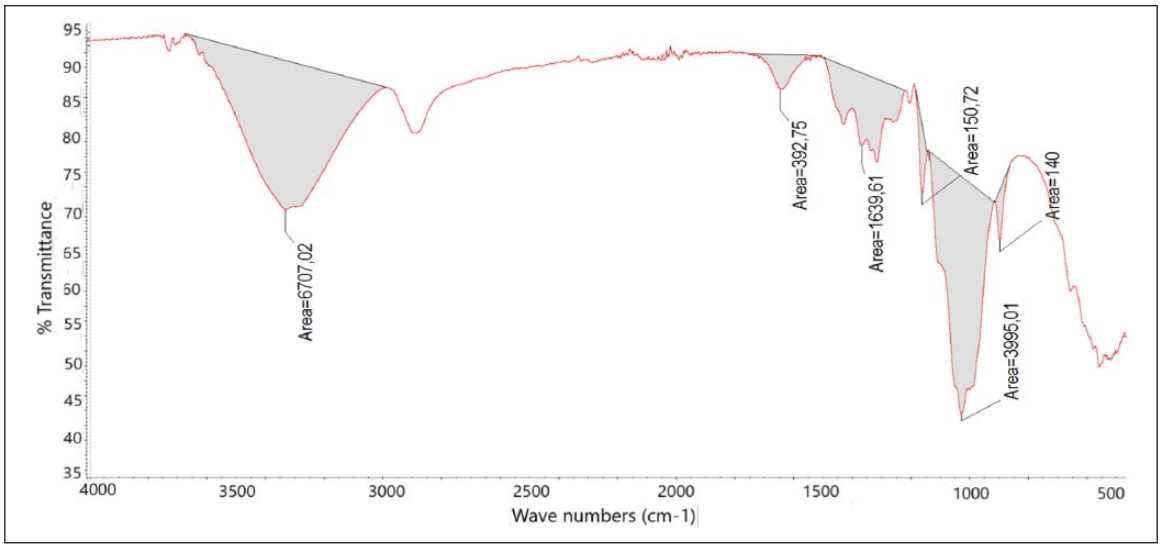

Figure 7. The places of measured peak area on the FTIR spectra of all samples.

Table 9. Area value of peak area which was assumed to be changed with altering process parameters.

Samples	Peak area at 3331 cm^{-1}	Peak area at 1637 cm^{-1}	Peak area at 1455–1313 cm^{-1}	Peak area at 1159 cm^{-1}	Peak area at 1021 cm^{-1}	Peak area at 896 cm^{-1}	Peak height at 1105 cm^{-1}
Cellulose 1	6680	412	1658	204	3991	144	25
Cellulose 2	6017	366	1549	187	3931	142	25
Cellulose 3	5843	337	1557	202	4124	142	26
Cellulose 4	5918	366	1486	188	3856	133	26
Cellulose 5	4879	315	1304	178	3683	119	22
Cellulose 6	5233	327	1370	184	3705	124	23
Cellulose 7	6000	387	1531	188	3968	140	25
Cellulose 8	6347	382	1617	202	4174	144	27
Cellulose 9	4866	299	1249	166	3455	113	21
Cellulose 10	5235	319	1349	177	3508	123	22

in the cellulose macromolecule.[31] Similar decrease with temperature increase could be seen on the peak area between 1455 and 1313 cm^{-1} of the FTIR spectra. The area of the peak at 1159 cm^{-1} decreases with increasing process temperature which is nearly the same as the decrease in the peak area at 896 cm^{-1} and between 1455 and 1313 cm^{-1} on the FTIR spectra. These peak groups are also related to cellulose macromolecule and cellulose molecule in terms of H-C-H, H-O-C, H-C-C, and H-C-O bonds.[31,32] The area of the peak at 896 cm^{-1} was sorted in descending order as cellulose 1, 8, 2, 3, 7, 4, 6, 10, 5, and 9. The smallest area was 113 and the biggest area was 144. The sequence was nearly the same as the peak area at 896 cm^{-1} in case of peak area between 1455 and 1313 cm^{-1}. The smallest area was 1249 and the biggest area was 1658. The ranking of the area at 1159 cm^{-1} was cellulose 1, 8, 3, 7, 4, 2, 6, 5, 10, and 9. The smallest area was 166 and the biggest area was 204. There was not a good regression in the relation of the chain breakage and temperature increase, due to that cellulose includes big variance consequence of being natural fiber and the process parameter could not be controlled as it should be. The results of FTIR spectra analysis show that there was no ring-opening reaction on the cellulose group, but there may be chain breakage in the cellulose macromolecule and there was water lost from cellulose molecular structure in the case of heating nanocellulose fiber. The change in the cellulose molecular structure depends on both process parameters—temperature and time (Table 9).

TGA results

TGA thermogram of all samples includes three thermal weight loss point (Figures 8 and 9). The first one was between beginning temperature and 120°C. This thermal event was related with loss of water molecule, which was in the fiber structure. The second mass loss point was related to the decomposition of the fiber. Thermal decomposition between beginning and endpoint change depends on samples (Table 10). The decomposition at beginning

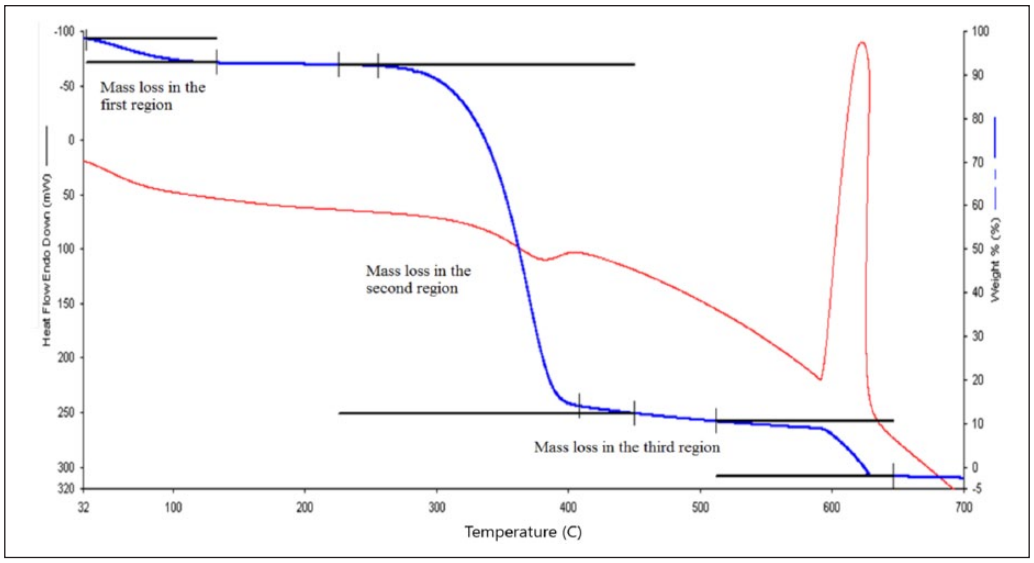

Figure 8. The places of measured peak point on the TGA thermogram of all samples.

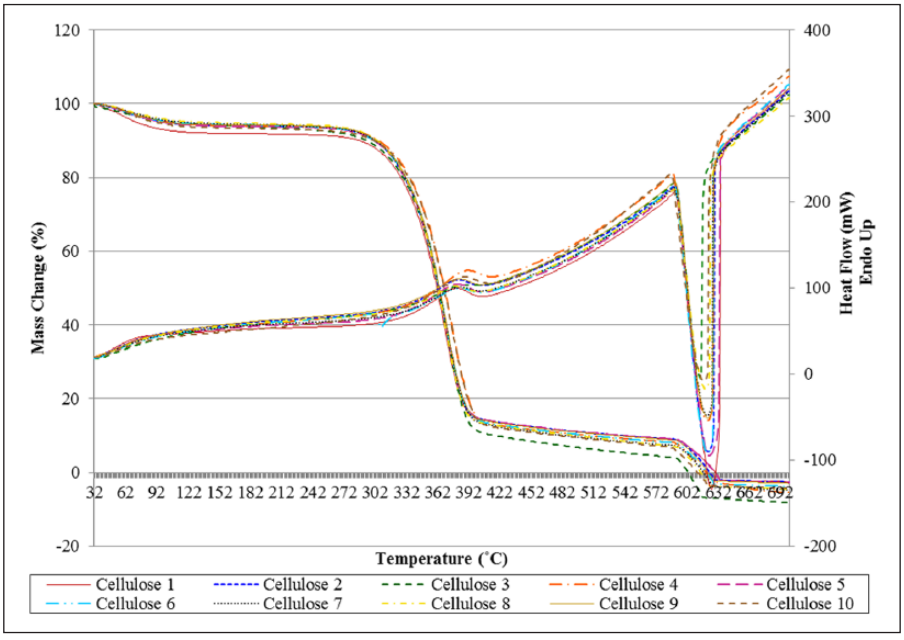

Figure 9. TGA thermogram of all samples.

temperature was sorted in descending order as cellulose 8, 4, 10, 2, 5, 3, 1, 7, 9, and 6. The lowest temperature was 231°C and the highest temperature was 266°C. The sequences from high to low value according to decomposition endpoint temperature of cellulose samples were cellulose 3, 4, 6, 9, 5, 10, 7, 1, 8, and 2. The lowest temperature was 408°C and the highest temperature was 444°C. The difference between the highest and lowest temperatures was 35°C for the beginning point and 36°C for the endpoint. These big differences show that the molecular structure of cellulose was affected by temperature change in the process. Beginning of the decomposition temperature is related to molecular weight. The lower molecular weight implies the lower beginning temperature.[33] It can be said from TGA thermogram that heating of the cellulose in high temperature during a period decreases the molecular weight of the cellulose. The amount of water loss was between 7.8% and 4.6%. Cellulose 1 involves more water than the others and the lowest water content belongs to cellulose 3. The ranking of samples according to water content was cellulose 1, 10, 5, 9, 2, 6, 7, 8, 4, and 3. These results show that all samples lose water during processing

Table 10. Thermal event on the thermograms.

Samples	Mass loss in the first region (%)	Mass loss in the second region (%)	Mass loss in the third region (%)	Second region mass loss beginning point (°C)	Second region mass loss endpoint (°C)
Cellulose 1	7	77	12	242.78	413.53
Cellulose 2	5.5	80	12.5	255.77	408.11
Cellulose 3	4.6	81.8	13.2	244.61	444.44
Cellulose 4	5	81.4	13.5	261.07	428.89
Cellulose 5	5.8	80.6	13.2	246.44	423.06
Cellulose 6	5.2	81.4	12.7	231.38	427.73
Cellulose 7	5.1	81.7	13.2	241.72	416.39
Cellulose 8	5.1	81.3	13.6	266.2	411.19
Cellulose 9	5.6	80.9	13.5	241.39	425.03
Cellulose 10	6.2	81.2	12.4	259.24	422.68

under high temperature. This water loss is related to the moisture content of fiber. FTIR spectra also show water loss in the fiber during processing under high temperature. The amount of weight loss during decomposition was between 74.8% and 81.8%. Cellulose 1 lost less weight than the others did. More weight loss occurred in cellulose 3. Weight loss was similar to other samples except cellulose 1 which was not processed. There was no residue in case of all samples. The third one was related to decomposition of carbon black under oxygen atmosphere condition. This event occurred between 600°C and 700°C. Decomposition of organic matter caused carbon black formation. The amount of carbon black decomposition was similar to each other and was about 13%.

Conclusion

In this study, the yellowing tendency of cellulose powders used for textile coating was investigated. Effects of process temperature and period on yellowing behavior were researched using cellulose powder–coated polyester fabrics and dry pure cellulose powders. In order to investigate the effect of coating chemicals on yellowing, control-coated fabrics were prepared with stock paste without adding cellulose powder and they were cured at same conditions.

The yellowness–whiteness values taken by a UV-VIS spectrophotometer showed that while the yellowness rates increased, the whiteness values decreased as the temperature and duration of the curing increase. In cellulose powder–coated fabrics, the yellowness values increased dramatically at temperatures over 140°C and longer times than 5 min. However, the dependence of the yellowing on the increase in curing time is not as significant as on the increase in temperature. Similarly, yellowing values increased with the increase in curing temperature and period for control-coated fabrics but color differences were not high compared to cellulose powder–coated fabrics. Based on these results, it can be said that the yellowing is caused by the synergistic effect of both cellulose powders and coating chemicals.

Heat-treated cellulose powders were analyzed by TGA and FTIR technique for determining cause of yellowing, and according to TGA and FTIR analysis, cellulose powder samples lost moisture and cellulose macromolecule chain breakage occurred during heating process, but there was no evidence for ring opening of the cellulose macromolecules.

Acknowledgements

The authors would like to thank CHT Chemistry (Turkey), JRS Group (Germany), and Kırayteks Inc. (Turkey) for supplying coating chemicals, cellulose powders, and fabrics.

Declaration of conflicting interests

The author(s) declared no potential conflicts of interest with respect to the research, authorship, and/or publication of this article.

Funding

The author(s) received no financial support for the research, authorship, and/or publication of this article.

References

1. Sen AK. *Coated textiles: principles and applications*. 2nd ed. Boca Raton, FL: CRC Press, 2007, p. 246.
2. Fung W. *Coated and laminated textiles*, vol. 23. Cambridge: Woodhead Publishing, 2002, p. 416.
3. Akovali G. *Advances in polymer coated textiles*. Shawbury: Smithers Rapra, 2012, p. 500.
4. Lavoine N, Desloges I, Dufresne A, et al. Microfibrillated cellulose—its barrier properties and applications in cellulosic materials: a review. *Carbohydr Polym* 2012; 90: 735–764.
5. Lu P and Hsieh YL. Preparation and properties of cellulose nanocrystals: rods, spheres, and network. *Carbohydr Polym* 2010; 82(2): 329–336.
6. El-Fattah MA, Hasan AMA, Keshawy M, et al. Nanocrystalline cellulose as an eco-friendly reinforcing additive to polyurethane coating for augmented anticorrosive behavior. *Carbohydr Polym* 2018; 183: 311–318.
7. Willberg-Keyriläinen P, Vartiainen J, Harlin A, et al. The effect of side-chain length of cellulose fatty acid esters on

their thermal, barrier and mechanical properties. *Cellulose* 2017; 24(2): 505–517.
8. Salah SM. Application of nano-cellulose in textile. *J Textile Sci Eng* 2013; 3: 142.
9. https://www.jrs.eu/jrs_en/ (accessed 7 November 2018).
10. https://www.jelu-werk.com/ (accessed 7 November 2018).
11. Braun MA, Effenberger F and Hermanutz F. Low degree of substitution cellulosic textile coatings with improved physiological parameters. *Cellulose* 2014; 21(1): 803–812.
12. Kale BM, Wiener J, Militky J, et al. Dyeing and stiffness characteristics of cellulose-coated cotton fabric. *Cellulose* 2016; 23(1): 981–992.
13. d'Eon J, Zhang W, Chen L, et al. Coating cellulose nanocrystals on polypropylene and its film adhesion and mechanical properties. *Cellulose* 2017; 24(4): 1877–1888.
14. Brillard A, Habermacher D and Brilhac JF. Thermal degradations of used cotton fabrics and of cellulose: kinetic and heat transfer modeling. *Cellulose* 2017; 24: 1579–1595.
15. Szcześniak L, Rachocki A and Tritt-Goc J. Glass transition temperature and thermal decomposition of cellulose powder. *Cellulose* 2008; 15(3): 445–451.
16. Teodorovic M, Majdanac L, Cosic D, et al. The thermal behaviour of cellulose samples with different structure. *J Thermal Anal Calori* 1992; 38(4): 907–916.
17. Lobo H and Bonilla JV. *Handbook of plastics analysis*. New York: Marcel Dekker, 2003, pp. 83–338.
18. Matheus P, Heitor LOJ and Ademir JZ. Native cellulose: structure, characterization and thermal properties. *Materials* 2014; 7: 6105–6119.
19. Jiangtao S, Dong X and Jian L. FTIR studies of the changes in wood chemistry from wood forming tissue under inclined treatment. *Energ Proc* 2012; 16: 758–762.
20. Åkerholm M, Hinterstoisser B and Salmén L. Characterization of the crystalline structure of cellulose using static and dynamic FT-IR spectroscopy. *Carbohydr Res* 2004; 339: 569–578.
21. Michał D, Janusz Z, Tomasz Z, et al. The influence of method of cellulose isolation from wood on the degree and index of crystallinity. *Wood Res* 2015; 60(2): 255–262.
22. Michael FF and Robert N. The interaction of water with cellulose from nuclear magnetic resonance relaxation times. *Macromolecules* 1975; 8(6): 726–730.
23. Tatsuko H, Yoshimitsu I and Hyoe H. Effect of bound water on structural change of regenerated cellulose. *Macromol Chem Phys* 1987; 188(8): 1875–1884.
24. Yongliang L, Devron T, Gary G, et al. Comparative investigation of Fourier transform infrared (FT-IR) spectroscopy and X-ray diffraction (XRD) in the determination of cotton fiber crystallinity. *Appl Spectro* 2012; 66(8): 983–986.
25. Popescu MC, Popescu CM, Lisa G, et al. Evaluation of morphological and chemical aspects of different wood species by spectroscopy and thermal methods. *J Mol Struct* 2011; 988: 65–72.
26. Yue Y. *A comparative study of cellulose I and II fibers and nanocrystals*. Master's Thesis, Louisiana State University, Baton Rouge, LA, 2007.
27. Harris M. *Handbook of textile fibers*. Washington, DC: Interscience Publishers, 1954, pp. 226–253.
28. Garner W. *Textile laboratory manual*. 3rd ed. New York: Elsevier, 1966.
29. Socrates G. *Infrared and Raman characteristic group frequencies tables and charts*. 3rd ed. Hoboken, NJ: John Wiley & Sons. 2011, pp. 15–145.
30. Calahorra ME, Cortázar M, Eguiazábal JI, et al. Thermogravimetric analysis of cellulose: effect of the molecular weight on thermal decomposition. *J Appl Polym Sci* 1989; 37(12): 3305–3314.
31. Cho LL. Identification of textile fiber by Raman microspectroscopy. *Foren Sci J* 2007; 6: 55–62.
32. Chargot MS, Cybulska J and Zdunek A. Sensing the structural differences in cellulose from apple and bacterial cell wall materials by Raman and FT-IR spectroscopy. *Sensors* 2011; 11: 5543–5560.
33. Haafiz MKM, Eichhorn SJ, Hassan A, et al. Isolation and characterization of microcrystalline cellulose from oil palm biomass residue. *Carbohydr Polym* 2013; 93: 628–663.